NASA TECHNICAL MEMORANDUM

NASA TM X-73682

NASA TM X-73682

(NASA-TM-X-73682) THERMOCHEMICAL ANALYSES OF THE OXIDATIVE VAPORIZATION OF METALS AND OXIDES BY OXYGEN MOLECULES AND ATOMS (NASA) 25 p HC A02/MF A01 CSCL 11F

N77-26270

Unclas
G3/26 35464

THERMOCHEMICAL ANALYSES OF THE OXIDATIVE VAPORIZATION OF METALS AND OXIDES BY OXYGEN MOLECULES AND ATOMS

by Fred J Kohl, Denise M. Leisz,
George C. Fryburg, and Carl A. Stearns
Lewis Research Center
Cleveland, Ohio 44135

TECHNICAL PAPER presented at the
Symposium on Corrosion Problems Involving Volatile Corrosion Products
sponsored by the Electrochemical Society
Philadelphia, Pennsylvania, May 8-13, 1977

THERMOCHEMICAL ANALYSES OF THE OXIDATIVE VAPORIZATION OF METALS AND OXIDES BY OXYGEN MOLECULES AND ATOMS

by Fred J. Kohl, Denise M. Leisz, George C. Fryburg, and Carl A. Stearns

National Aeronautics and Space Administration
Lewis Research Center
Cleveland, Ohio 44135

ABSTRACT

Equilibrium thermochemical analyses are employed to describe the vaporization processes of metals and metal oxides upon exposure to molecular and atomic oxygen. The effect of adding atomic oxygen to a system is equivalent to increasing the chemical potential of oxygen. As a consequence, enhanced oxidation in oxygen atoms should be exhibited by any metal or oxide for which there exists a stable, gaseous oxide of high volatility with the metal atom in a higher oxidation state. Specific analytic results for the chromium-, platinum-, aluminum-, and silicon-oxygen systems are presented. Maximum rates of oxidative vaporization predicted from thermochemical considerations are compared with experimental results for chromium and platinum. The oxidative vaporization rates of chromium and platinum are considerably enhanced by oxygen atoms. For the aluminum system, the AlO_2 molecule should lead to enhanced vaporization of the Al_2O_3 phase. However, the magnitude of the predicted enhancement is small compared to those for chromium or platinum. In the silicon system, SiO(g) should lead to enhanced vaporization of the silicon phase, whereas the SiO_2 condensed phase can be unaffected or even somewhat stabilized by oxygen atoms.

E-9032

STAR Category 26

INTRODUCTION

The active use of "near space" envisioned for the 1980's and beyond has revived interest in the interaction of oxygen atoms in the gas phase with metals and metal oxides. Of particular interest is the ambient environment of the space shuttle spacelab. At the proposed shuttle orbit of about 450 km, oxygen atoms are the main elemental constituent. The relatively large atomic oxygen flux resulting from these atoms suggests the possibility of both destructive interactions with materials and the opportunity to perform interesting surface oxidation experiments.

Some years ago, one of us demonstrated that oxygen atoms (O) caused a marked enhancement in the rate of oxidation of platinum (Refs. 1,2) compared with the oxidation by molecular oxygen (O_2). Subsequently, Rosner and Allendorf (Refs. 3-6) extended these studies to molybdenum, tungsten, boron, rhenium, and graphite, obtaining similar enhancements in the rates of oxidation. Madix (Ref. 7), using atomic beam techniques, found an enhanced oxidation of germanium and silicon with oxygen atoms. All of these metals form volatile oxides in the temperature range in which the enhanced oxidation was discovered. This type of oxidation of metals in which volatile oxides are formed is classified as oxidative vaporization. More recently, we showed (Ref. 8) that both chromium metal and chromium sesquioxide (Cr_2O_3) underwent enormously enhanced oxidative vaporization upon interaction with oxygen atoms when compared with oxygen molecules. We believe that this was the first example of enhanced oxidation of a metal oxide by oxygen atoms.

Because metal-oxygen systems such as those mentioned above are numerous, a method of elucidating the chemical reactions and predicting rates of oxidative vaporization from equilibrium thermodynamic data would be valuable. Jansson and Gulbransen (Refs. 9-13) have utilized equilibrium thermochemical volatility diagrams of the type described by Kellogg (Ref. 14) for a number of metal-oxygen molecule systems. They were able to predict and interpret oxidation and vaporization behavior. Recently, we have utilized thermochemical diagrams to describe the chemistry of both oxygen molecule

and atom oxidation of chromium and chromium sesquioxide (Refs. 8, 15). In the present paper, we review the application of thermochemical diagrams to the chromium-oxygen system and extend the treatment to the platinum-, aluminum-, and silicon-oxygen systems. The objective is to interpret the thermochemistry of oxidative vaporization and to predict kinetic behavior (i.e., rates of vaporization) from established thermochemical data.

THERMOCHEMICAL ANALYSES

To describe quantitatively the equilibrium mode of vaporization of a metal and its oxides in various oxidizing atmospheres, one must know the partial pressures of all vapor species involved as a function of condensed phase composition, temperature, and oxygen pressure. For the four metal-oxygen systems under consideration, thermochemical diagrams were constructed following the methods outlined by Jansson and Gulbransen (Ref. 9). The individual metal-oxygen systems will be discussed individually below. In general, the diagrams show both (1) the relationship between condensed phases and (2) the vapor pressures of the various metal-oxygen-containing gaseous molecules as a function of either $O_2(g)$ or O(g) pressures at a specified temperature. For any individual reaction, the reaction order with respect to either $O_2(g)$ or O(g) is obtained from $d \log P_i / d \log P_{O_2}$ or $d \log P_i / d \log P_O$, where P_i is the vapor pressure of species i.[2] Also, from the respective diagrams at different temperatures, one can obtain the vapor pressure of each species as a function of temperature for any given oxygen pressure.

Thermochemical diagrams are calculated easily if values of log Kp are available for each condensed phase and gaseous molecule in the system under consideration. Log Kp stands for the logarithm of the equilibrium constant for the reaction of forming a given compound from its elements in their standard states. Values of log Kp are listed in thorough thermodynamic data compilations such as the JANAF Tables (Ref. 16);

they can be calculated from values of free energies of formation, $\log Kp = -\Delta G/RT$; or they can be obtained from heat capacity data for condensed phases or molecular parameters for gases by use of thermodynamic programs such as the NASA Program For Calculation of Thermodynamic Data (Ref. 17).

The partial vapor pressures of the molecular species can be calculated by consideration of the expression for the equilibrium constant in terms of the activities of reactants and products for the appropriate chemical reactions, and use of the relationship

$$\log K_{reaction} = \sum \log Kp,_{products} - \sum \log Kp,_{reactants} \qquad (1)$$

Previously, Fryburg and Petrus (Ref. 18) showed that kinetic data, obtained from a study of the oxidative vaporization of platinum, could be correlated with equilibrium thermodynamic data. It is useful to reverse this process and to predict kinetic behavior from thermodynamic data. The vapor pressures (P_i) given in the thermochemical diagrams may be used to calculate the equilibrium or maximum possible rate of vaporization of any species, i. The Hertz-Langmuir equation is then used to calculate the rate of weight loss of metal, $\dot{m}_{metal}$, by

$$\dot{m}_{metal}(gm\text{-}cm^{-2}\text{-}sec^{-1}) = 44.35\ P_i(atm)\ \frac{M_{metal}}{M_i^{1/2}T^{1/2}} \qquad (2)$$

where M_{metal} is the molecular weight of the metal and M_i is the molecular weight of the vaporizing molecule. If more than one vaporizing species is important the individual values of $\dot{m}$ must be summed to obtain the total weight loss.

The slope of a plot of $\log P_i$ versus T^{-1} for a given reaction can be used to obtain the enthalpy ΔH for the reaction:

$$\text{slope} = \frac{-\Delta H_T}{R \ln 10} \tag{3}$$

The experimental energy of activation obtained from a plot of $\log \dot{m}$ versus T^{-1} is related to the enthalpy (Ref. 15) by

$$E_{act} = \Delta H_T - \frac{RT}{2} \tag{4}$$

Thus thermochemical considerations can be used to predict E_{act}, a kinetic quantity.

CHROMIUM-OXYGEN SYSTEM

Thermochemical diagrams for the chromium-molecular oxygen system at 800 and 1500 K are given in Figures 1 and 2 and for the chromium-atomic oxygen system in Figures 3 and 4. The thermodynamic data used to construct these diagrams are given in Ref. 8. For the molecular oxygen case the important molecular species in equilibrium with $Cr_2O_3(s)$ are $CrO_3(g)$ and $CrO_2(g)$ at O_2 pressures greater than 10^{-8} atm. At 800 K, $(CrO_3)_3(g)$ also becomes important at high O_2 pressures and at 1500 K $Cr_3O_7(g)$ becomes significant at pressures greater than 10^{-1} atm.

The atomic oxygen diagrams differ markedly from the molecular ones in several respects. In addition to Cr and Cr_2O_3 condensed phases, a CrO_3 condensed phase is present at high oxygen atom pressures. Whereas the complex chromium-oxygen molecules are relatively unimportant in the molecular oxygen case, the polymeric $(CrO_3)_n$ and Cr_nO_{3n-2} molecules ($n = 3, 4$, and 5) are the predominant species in the vapor phase at high oxygen atom pressures, particularly over the CrO_3 phase. In addition, the actual vapor pressures of the oxides are markedly higher in the atomic oxygen case. At 800 K comparison of the vapor pressure of $(CrO_3)_3$ under the oxygen atom partial pressure of 3.8×10^{-6} atm (the value of P_O used in

experiments reported in Ref. 8) with the vapor pressure of CrO_3 under a molecular oxygen partial pressure of 1.5×10^{-4} atm indicates an enhancement in oxide vapor pressure of about 10^{13}. The oxidative vaporization rate should be enhanced by a similar factor. At 1500 K the situation is a little different. Under the oxygen atom pressure of 3.8×10^{-6} atm, the polymers of CrO_3 are not stabilized at this higher temperature and the main oxide product is again the monomer, CrO_3. Comparison of the vapor pressure of CrO_3 from Fig. 4 at $P_{O} = 3.8\times10^{-6}$ atm with the vapor pressure from Fig. 2 at $P_{O_2} = 1.51\times10^{-4}$ atm, indicates an enhancement of about 10^2.

It is instructive to plot the vapor pressures of the various oxide species against T^{-1} for the molecular and atomic oxygen partial pressures under consideration. These plots are given in Figs. 5 and 6. For the molecular oxygen case, it is obvious that $CrO_3(g)$ is the major vapor product in the oxidative vaporization of $Cr_2O_3(s)$ over the entire temperature range considered. For the atomic oxygen case, the polymers of CrO_3 are stabilized over $CrO_3(\ell)$ and are the principal vapor species up to the Cr_2O_3-CrO_3 phase boundary at a temperature around 950° C. At temperatures above this, the pressure of the polymers decreases dramatically and the monomer of CrO_3 becomes the most abundant oxide species as in molecular oxygen. Because the rate of oxidative vaporization should vary with the vapor pressures, we conclude that the rate in oxygen atoms should increase with temperature to 950° C and then fall abruptly with increasing temperature.

For comparison with experimental rates (Refs. 8, 15) of oxidative vaporization of Cr_2O_3, rates have been calculated from the oxide vapor pressures obtained from the thermochemical diagrams using the Hertz-Langmuir equation (eq. (2)). The results are presented in Fig. 7. In the cases where more than one oxide species were significant, the rates were calculated for each species and the individual rates summed to give the total rate of oxidation. These rates correspond to "reaction controlled" conditions, uninhibited by mass transport through a boundary layer. Included in Fig. 7 are the experimental data reported in Refs. 8 and 15. The

calculated and experimental rates for the oxidative vaporization of Cr_2O_3 by O_2 agree within experimental error with rates calculated from the equilibrium thermodynamic data. The calculated and experimental rates in partially atomic oxygen are in qualitative agreement with the calculations; both indicate a marked enhancement in the oxidation rate and exhibit a maximum in the rate at intermediate temperatures. Nevertheless, there is a large difference in the values of the rates and in the temperature at which the maximum occurs. Both these factors are dependent on the concentration of oxygen atoms on the surface of Cr_2O_3. We believe the disparity arises from the fact that the concentration of oxygen atom on the surface during the experiments was much less than the equilibrium value corresponding to the gaseous partial pressure. This results from rapid recombination of the absorbed oxygen atoms on the hot surface. While it has been shown that Cr_2O_3 at room temperature has a very low recombination coefficient for oxygen atoms (Refs. 19, 20) the recombination coefficient increases rapidly with increasing temperature (Ref. 19). This might offer an explanation for the drop in the experimental rate at 550° C. However, we feel that destabilization of the CrO_3 polymers is a more plausible explanation as shown by the thermodynamic data.

It is interesting to consider the enhancement in the rate of oxidation of Cr_2O_3 affected by a small concentration of oxygen atoms in the gas phase. The enhancements have been calculated at different temperatures from the results given in Fig. 7, and are presented in Fig. 8. We present here the enhancement calculated from both the experimental and the calculated rates. The enhancements are truly enormous at the lower temperatures, the experimental values being 10^{20} at 200° C and 10^{9} at 550° C. At 1000° C the enhancement is 100. Of course, with larger concentrations of oxygen atoms, the enhancements would be even greater.

PLATINUM-OXYGEN SYSTEM

Thermochemical diagrams for the platinum-molecular oxygen system at 1400 and 2000 K are given in Figs. 9 and 10 and for the platinum-atomic oxygen system in Figs. 11 and 12. The thermodynamic data used to construct these diagrams were obtained from the literature as follows: PtO_2(s), Pt_3O_4(s), Ref. 21; Pt(g), Ref. 22; PtO(g), Ref. 23; and PtO_2(g), Ref. 24. For the molecular oxygen case the important gaseous species are Pt, PtO, and PtO_2 over Pt(s) and only PtO_2 over Pt_3O_4(s) and PtO_2(s). * It is evident that condensed phase platinum-oxides are only stable at relatively high oxygen pressures.

In contrast to the chromium system, the atomic oxygen diagrams differ only slightly from the molecular ones. Again the Pt, PtO, and PtO_2 appear to be important over Pt(s) while PtO_2 predominates over Pt_3O_4(s) and PtO_2(s). The effect of atomic oxygen is to move the stability regions for Pt_3O_4(s) and PtO_2(s) to considerably lower oxygen pressures. On the whole, the platinum-oxygen system is much simpler than the chromium-oxygen because of the relative paucity of stable gas molecules.

---

*The existence of PtO_3(g) as the major Pt-oxygen-containing molecule at high P_{O_2} has been reported by Olivei (Ref. 25). We question his results and submit that he was observing a molecule other than PtO_3 in his mass spectrometric observations. If PtO_3 is considered in the thermochemical treatment the results give very high platinum molecule pressures under moderate and high O_2 pressures at low temperatures. The high pressures lead to high rates of Pt vaporization. These results are not in agreement with any of the other experimental observations on the oxidative vaporization of platinum (Refs. 18 and 23 and refs. contained therein). Indeed, in experiments carried out in this laboratory, we have observed PtO_2(g) by high pressure sampling mass spectrometry over platinum at 1150° C in one atmosphere of O_2. PtO_3(g) was not observed.

In Figs. 13 and 14 the vapor pressures of the Pt-O molecules are plotted versus T^{-1} for a molecular oxygen pressure of 6.58×10^{-4} atm and an atomic oxygen pressure of 4.61×10^{-5} atm, respectively. The particular O_2 and O pressures are chosen because these are the experimental conditions employed by Fryburg (Refs. 1 and 2) in investigations of the kinetics of oxidation of platinum. For both cases it is apparent that $PtO_2(g)$ is the predominant vapor species up to ~2000 K where the Pt and PtO pressures become comparable.

The results of the calculation of the rates of oxidative vaporization are given in Fig. 15 along with the experimental results of Fryburg (Refs. 1 and 2). The agreement between the calculated and experimental rates for molecular oxygen is excellent. However, the experimental rates for the partially atomic oxygen situation fall considerably below the calculated values. The calculated and experimental values of the oxygen atom enhancements are shown in Fig. 16 where the experimental values are again shown to fall considerably below the calculated. We feel that the lack of better agreement is probably due to the large amount of oxygen atom recombination on platinum (Ref. 26) which results in a much lower concentration of atoms on the surface than the equilibrium value corresponding to the partial pressure. Nonetheless both the calculated and experimental results demonstrate that O atoms lead to enhanced oxidative vaporization of platinum and stabilize the $Pt_3O_4(s)$ and $PtO_2(s)$ phases.

ALUMINUM-OXYGEN SYSTEM

A thermochemical diagram for the aluminum-molecular oxygen system at 1800 K is given in Fig. 17 and for the aluminum-atomic oxygen system in Fig. 18. The thermodynamic data used to construct these diagrams were obtained from the JANAF Tables (Ref. 16) except for $Al_2(g)$ (Ref. 27). The diagrams have a similar appearance at all temperatures between 1000 and 2400 K. Over the $Al(\ell)$ phase the major vapor species are Al(g), $Al_2(g)$.

and $Al_2O(g)$. Over the $Al_2O_3(s)$ phase Al(g) and $Al_2O(g)$ are the major species at low pressures near the $Al\text{-}Al_2O_3$ phase boundary, but at higher O_2 or O pressures $AlO_2(g)$ and AlO(g) predominate.

In Figs. 19 and 20 the vapor pressures of the main Al-containing molecules are plotted versus T^{-1} for a molecular oxygen pressure of 0.1 atm and an atomic oxygen pressure of 1×10^{-2} atm. These pressures were chosen arbitrarily because no experimental data for comparison are available. The calculated oxidative vaporization rates are given in Fig. 21. The vaporization of Al at the specified pressures is due mainly to the AlO_2 molecule. The calculated enhancement of the oxidative vaporization rate is given in Fig. 22. At low temperatures the enhancement is large, about 10^4 at 1000 K, but drops to less than a factor of 10 at 2000 K. Although reasonably large enhancements are calculated for the lower temperatures, the absolute rates of vaporization are very low when considered on a practical basis. The rates of vaporization would probably be of practical significance only above temperatures of 1700 K, where the enhancement is around 10.

SILICON-OXYGEN SYSTEM

A thermochemical diagram for the silicon-molecular oxygen system at 1800 K is given in Fig. 23 and for the silicon-atomic oxygen system in Fig. 24. All of the thermodynamic data were taken from the JANAF Tables (Ref. 16).

The most striking feature evident in these diagrams is the high vapor pressure of SiO(g) at the $Si(\ell)$ - $SiO_2(s)$ phase boundary where the equilibrium oxygen pressures are quite low. This circumstance strongly influences the kinetics and mechanism of oxidation for elemental silicon. Under equilibrium conditions at high oxygen pressures (10^{-4} to 1 atm) both SiO(g) and $SiO_2(g)$ are vaporization products with fairly low vapor pressures. However, the high SiO(g) pressure at the metal-oxide interface can be a cause of problems in practical systems. For example, if a surface oxide coating is porous, SiO(g) can rapidly diffuse to the surface where it can either vaporize or form

SiO_2 smoke by reaction with oxygen. Alternately the high SiO(g) pressure at the interface may lead to cracking and rupture of the surface if the external total pressure is lower than that of the SiO(g). The pressures (and diffusion coefficients) of SiO(g) and oxygen also determine the transition between so called active (rapid) and passive (slow) oxidation. In general, a passive SiO_2(s) layer is formed if the oxygen pressure is greater than the SiO(g) pressure. Gulbransen and Jansson have previously considered many facets of the behavior of the silicon-molecular oxygen in the light of thermochemical analyses (Refs. 10, 13, 28).

For the silicon-oxygen atom case, the vapor pressure of SiO(g) is increased somewhat over a small O-pressure range over the Si(ℓ) phase. However, the O-pressures when this occurs are extremely low (i.e., less than 10^{-12} atm). Over SiO_2(s) at higher O pressures (10^{-10} to 1 atm) the SiO_2(g) vaporization is pressure independent, and the vapor pressure of SiO(g) is decreasing with increasing O pressure. Thus the net result of going from molecular to atomic oxygen is a slight decrease in total pressure of silicon-containing species. Since no enhancement of vaporization of silicon can be envisioned here no enhancement diagrams were constructed for this system.

CONCLUDING REMARKS

In summary, we have shown that equilibrium thermochemical diagrams can be useful in interpreting the chemistry of metal-oxygen systems and in analyzing the rates of oxidative vaporization under specified molecular and atomic oxygen pressures. The effect of adding atomic oxygen is equivalent to increasing the chemical potential of oxygen. Enhanced oxidative vaporization should be exhibited by any metal or oxide for which there exists a stable gaseous oxide of high volatility with the metal in a higher valence state. It has been shown that oxygen atoms markedly enhance the oxidative vaporization of Cr_2O_3. Indeed, the magnitude of this effect can be important in engineering applications. The vaporization of platinum is also enhanced by

oxygen atoms but to a lesser degree than Cr_2O_3. The $AlO_2(g)$ molecule should lead to enhanced vaporization of Al_2O_3 with oxygen atoms, but the magnitude of the predicted enhancement is small compared to those for Cr_2O_3 or platinum. At temperatures where the AlO_2 vapor pressures are significant the enhancement is minimal. Therefore under most practical conditions, enhanced oxidative vaporization of Al_2O_3 would not be a problem. In the silicon system, SiO(g) should lead to enhanced vaporization of the silicon phase (a process which takes place only at very low oxygen pressure), whereas the SiO_2 condensed phase can be unaffected or even somewhat stabilized by oxygen atoms.

Other systems which fulfill the criteria for enhanced vaporization by oxygen atoms are the following:

$B_2O_3(s) \longrightarrow BO_2(g)$

$U_3O_8(s) \longrightarrow UO_3(g)$

$UO_2(s) \longrightarrow UO_3(g)$

$IrO_2(s) \longrightarrow IrO_3(g)$

$C(s) \longrightarrow CO, CO_2(g)$

$W(s) \longrightarrow WO_3(g)$

$ReO_2(s) \longrightarrow Re_2O_7(g)$

$ReO_3(s) \longrightarrow Re_2O_7(g)$

$Mn_2O_3(s) \longrightarrow Mn_2O_7(g)$

$MnO_3(s) \longrightarrow Mn_2O_7(g)$

$V_2O_3(s) \longrightarrow V_4O_{10}(g)$

$Mo(s) \longrightarrow MoO_3(g)$

Thermochemical analyses should prove useful in interpreting the chemistry and kinetics for these systems.

REFERENCES

1. G. C. Fryburg, J. Chem. Phys., 24, 175 (1956)

2. G. C. Fryburg, J. Phys. Chem., 69, 3660 (1965).

3. D. E. Rosner and H. D. Allendorf, J. Electrochem. Soc., 114, 305 (1967).

4. D. E. Rosner and H. D. Allendorf, in "Proceedings of the Third International Symposium on High Temperature Technology," p 707, London, Butterworths (1967).

5. D. E. Rosner and H. D. Allendorf, J. Chem. Phys., 49, 5553 (1968).

6. D. E. Rosner and H. D. Allendorf, AIAA J., 3, 1522 (1965).

7. R. J. Madix and A. A. Susu, Surface Sci., 20, 377 (1970).

8. G. C. Fryburg, F. J. Kohl, and C. A. Stearns, J. Electrochem. Soc., 121, 952 (1974).

9. S. A. Jansson and E. A. Gulbransen, in "Proceedings of the Fourth International Congress on Metallic Corrosion," N. E. Hammer, Editor, p. 331, Nat. Assoc. Corros. Eng., Houston, Tex. (1972).

10. E. A. Gulbransen and S. A. Jansson, in "Heterogeneous Kinetics at Elevated Temperatures", G. R. Belton and W. L. Worrell, Editors, p. 181, Plenum Press, New York (1970).

11. E. A. Gulbransen, Corrosion-NACE, 26, 19 (1970).

12. S. A. Jansson, J. Vacuum Sci. Technol., 7, S5 (1970).

13. E. A. Gulbransen and S. A. Jansson, in "Oxidation of Metals and Alloys," pp. 63-89, American Society for Metals, Metals Park, Oh (1971).

14. H. H. Kellogg, Trans. Metall. Soc. AIME, 236, 602 (1966).

15. C. A. Stearns, F. J. Kohl, and G. C. Fryburg, J. Electrochem. Soc., 121, 945 (1974).

16. JANAF Thermochemical Tables, Dow Chemical Co., Midland, Michigan.

17. B. J. McBride and S. Gordon, NASA TN D-4097 (1967).

18. G. C. Fryburg and H. M. Petrus, J. Electrochem. Soc., 108, 496 (1961).

19. P. G. Dickens and M. S. Sutcliff, Trans. Faraday Soc., 60, 1272 (1964).

20. C. D. Scott, NASA TN D-7113 (1973).

21. O. Muller and R. Roy, J. Less-Common Metals, 16, 129 (1968).

22. H. L. Schick, Editor, "Thermodynamics of Certain Refractory Compounds", Academic Press, N. Y. (1966).

23. J. H. Norman, H. G. Staley, and W. E. Bell, J. Phys. Chem., 71, 3686 (1967).

24. C. B. Alcock and G. W. Hooper, Proc. Roy-Soc., A254, 551 (1960).

25. A. Olivei, J. Less-Common Metals, 29, 11 (1972).

26. G. C. Fryburg and H. M. Petrus, J. Chem. Phys., 32, 622 (1960).

27. C. A. Stearns and F. J. Kohl, High Temp. Sci., 5, 113 (1973).

28. E. A. Gulbransen and S. A. Jansson, Oxid. Metals, 4, 181 (1972).

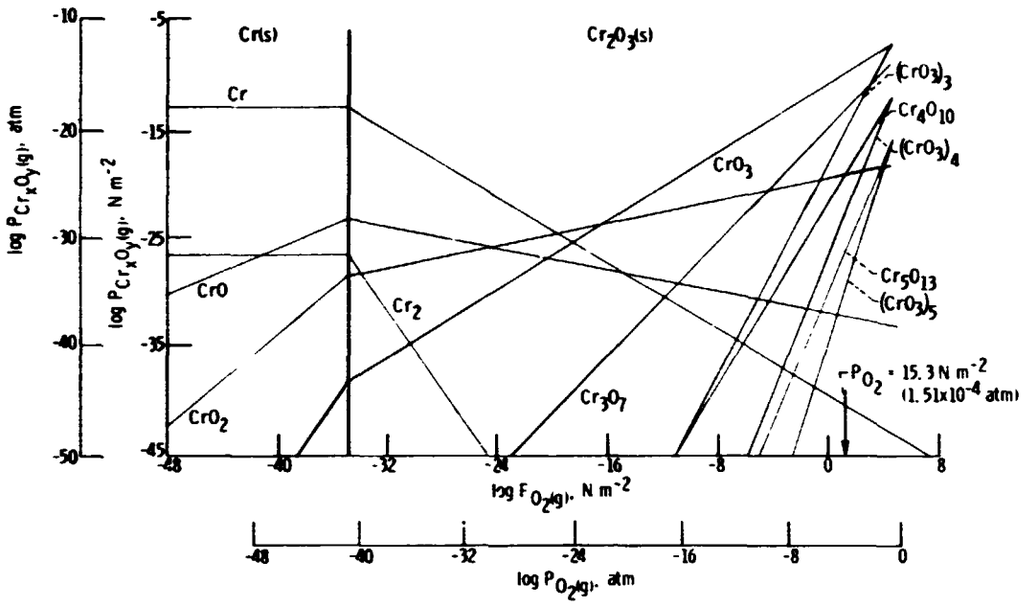

Figure 1. - Equilibrium thermochemical diagram for the chromium-oxygen system at 800 K. Arrow indicates experimental oxygen pressure of 1.51x10^{-4} atm used in reference 15.

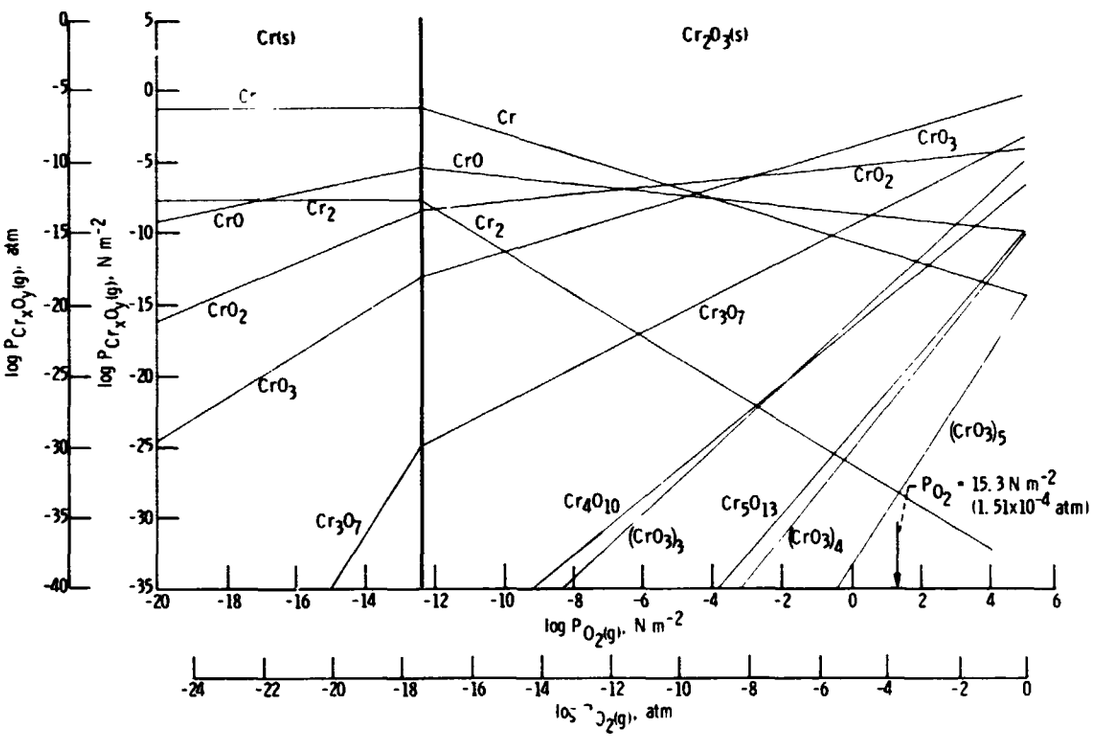

Figure 2. - Equilibrium thermochemical diagram for the chromium-oxygen system at 1500 K. Arrow indicates experimental oxygen pressure of 1.51x10^{-4} atm used in reference 15.

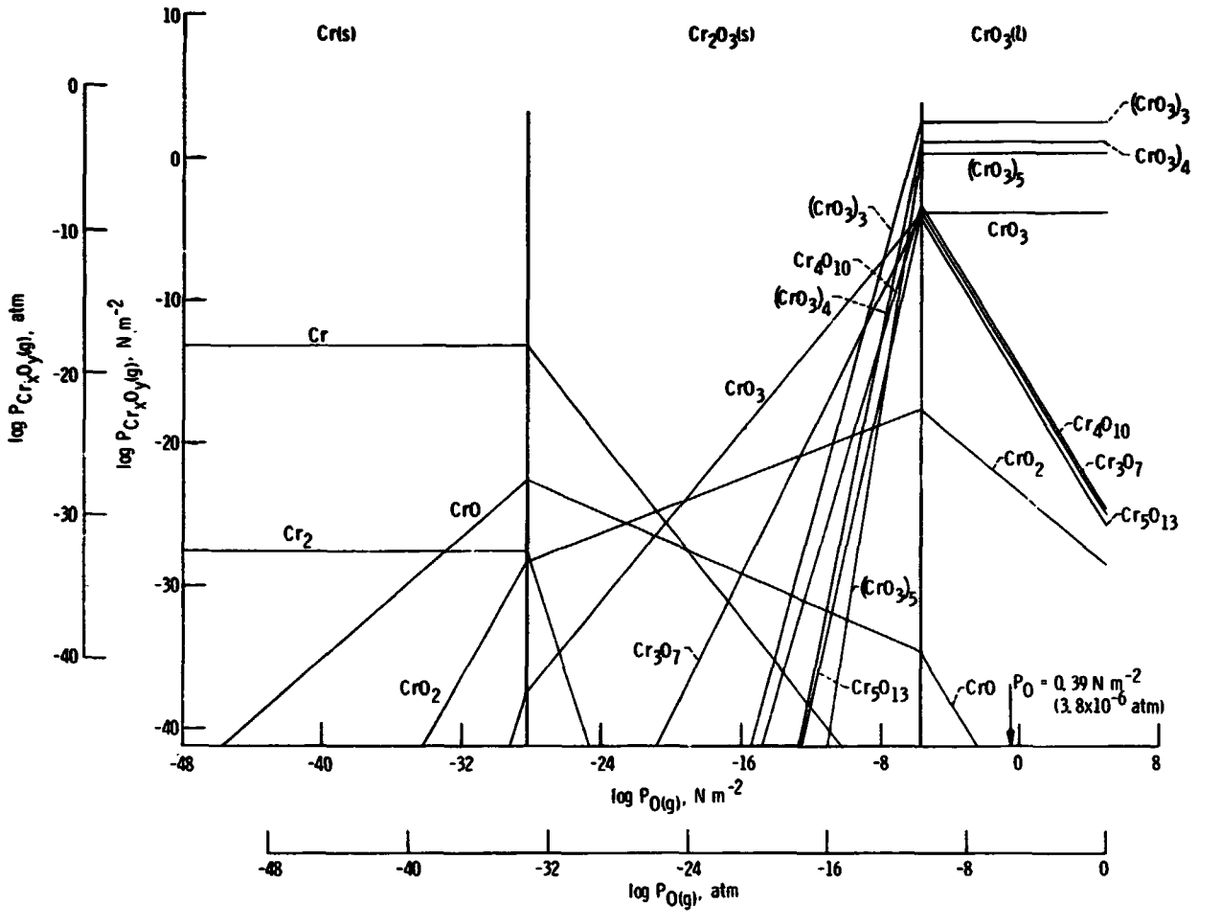

Figure 3. - Equilibrium thermochemical diagram for the chromium-atomic oxygen system at 800 K. Arrow indicates experimental oxygen atom partial pressure of 3.8x10^{-6} atm used in reference 8.

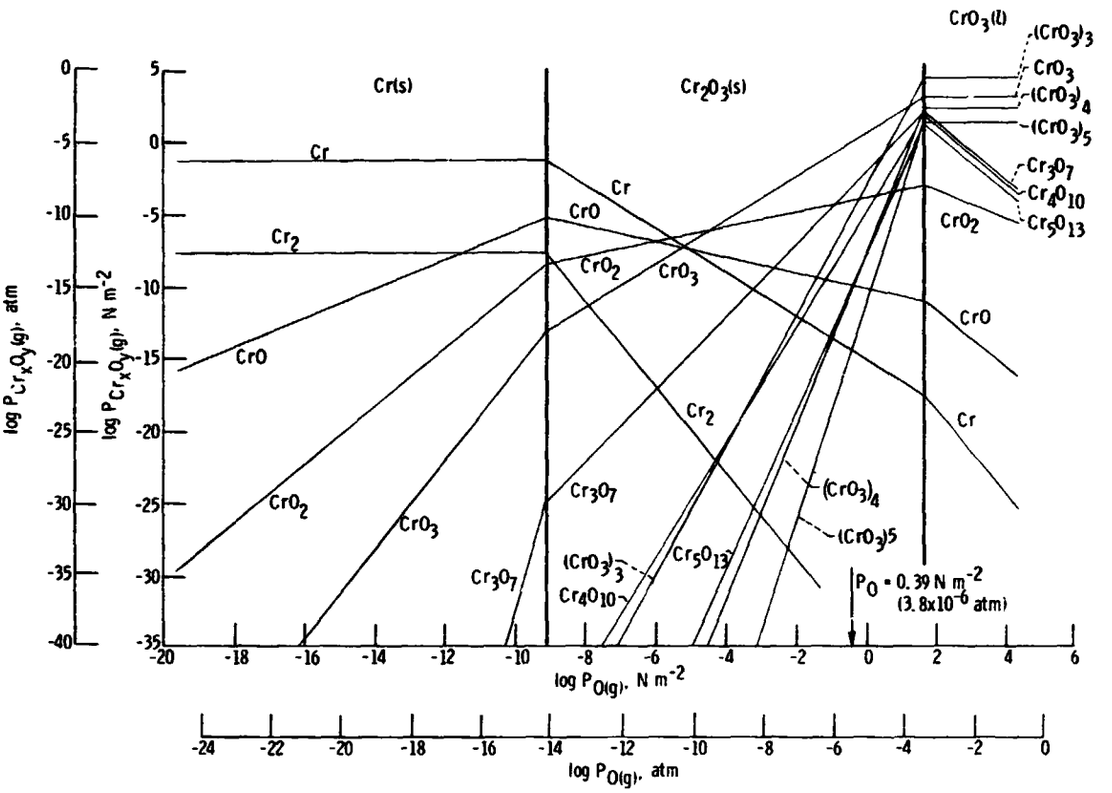

Figure 4. - Equilibrium thermochemical diagram for the chromium-atomic oxygen system at 1500 K. Arrow indicates experimental oxygen atom partial pressure of 3.8x10^{-8} atm used in reference 8.

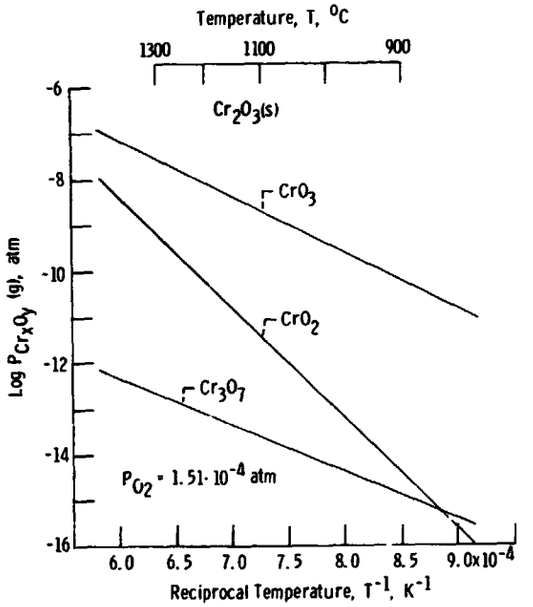

Figure 5. - Equilibrium vapor pressures of various oxide species of the chromium-oxygen system over Cr_2O_3(s) vs T^{-1} under an oxygen pressure of 1.51x10^{-4} atm.

NASA-Lewis-Com'l

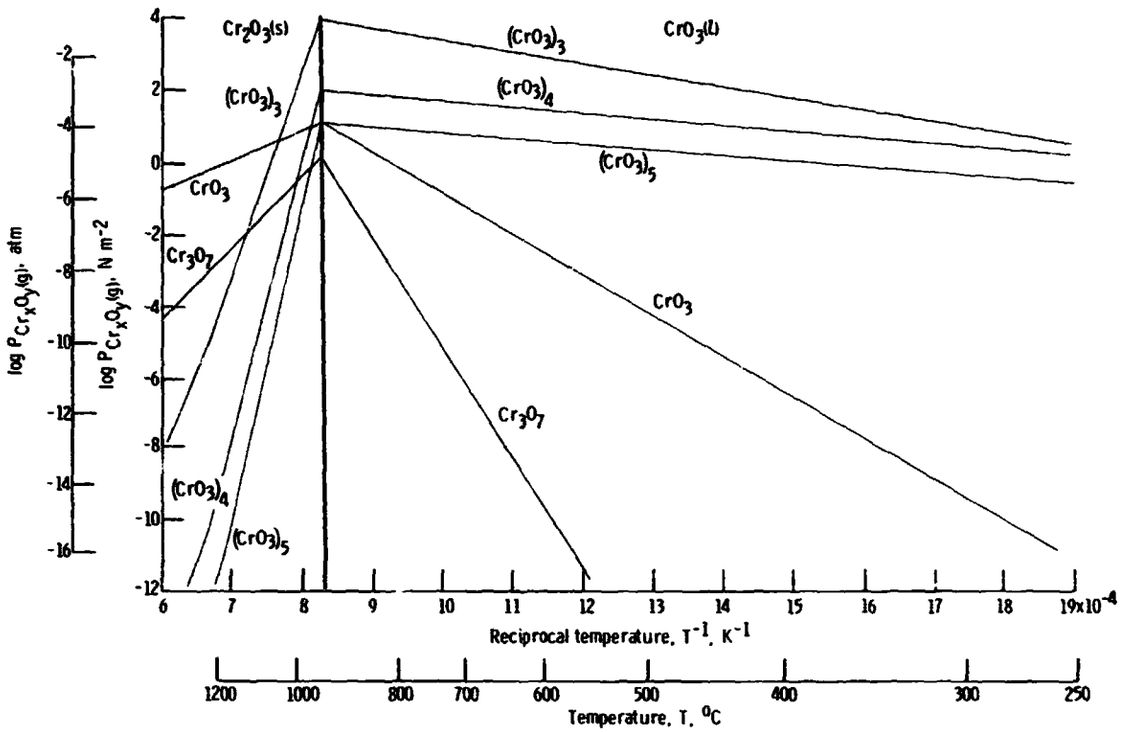

Figure 6. - Equilibrium vapor pressures of various oxide species of the chromium-atomic oxygen system vs T^{-1} under an oxygen atom partial pressure of 3.8×10^{-6} atm.

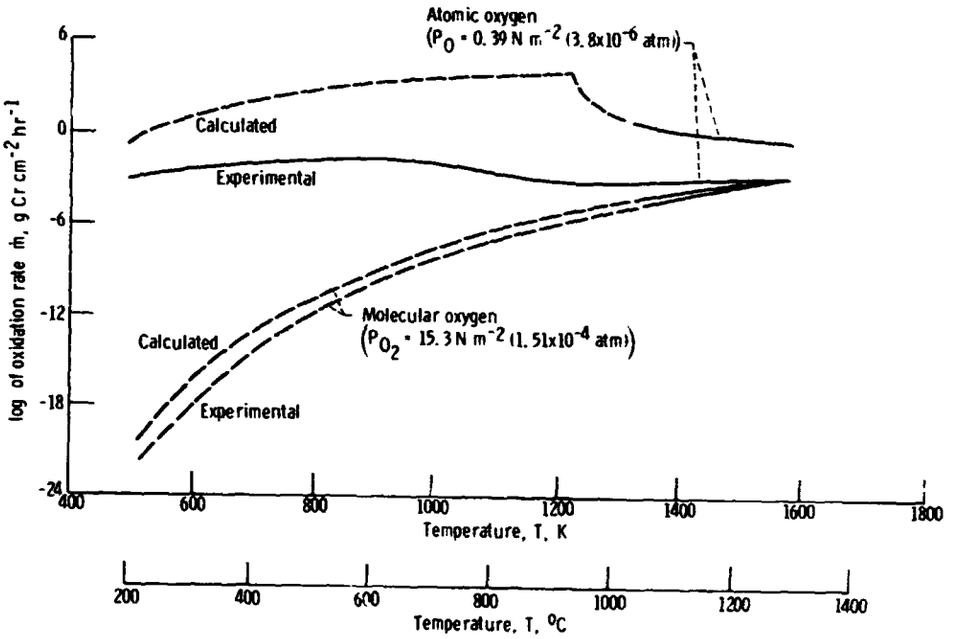

Figure 7. - Experimental and calculated rates of oxidative vaporization of Cr_2O_3 in partially atomic and molecular oxygen. Dashed curves are extrapolated.

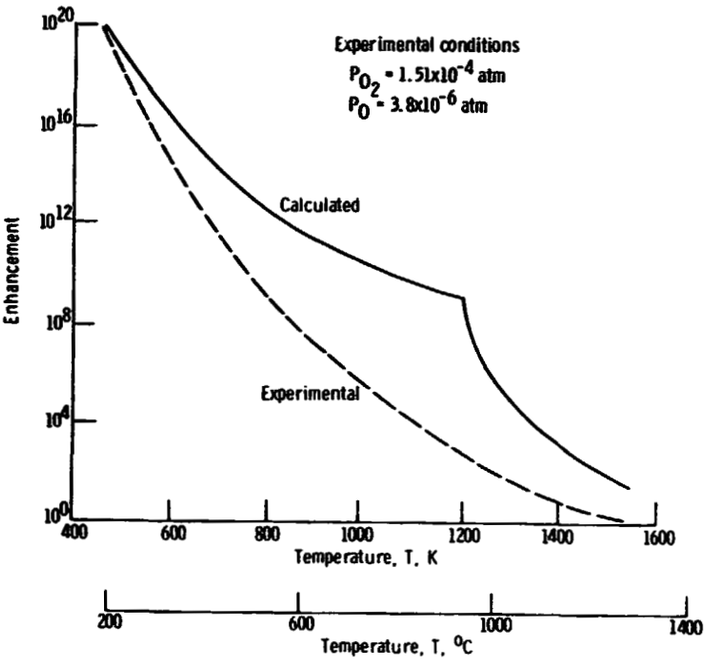

Figure 8. - Enhancement of oxidative vaporization of Cr_2O_3 in partially atomic oxygen.

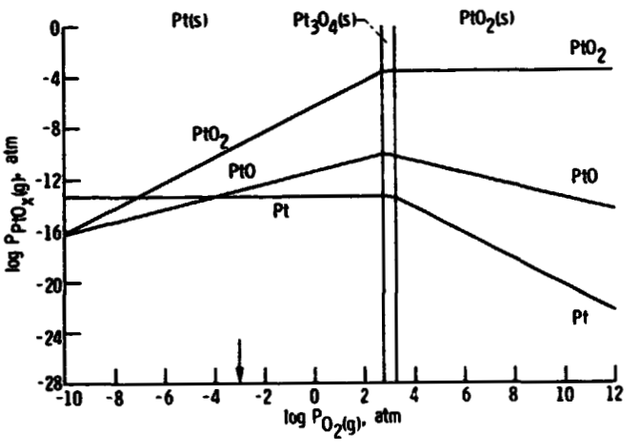

Figure 9. - Equilibrium thermochemical diagram for the platinum-oxygen system at 1400 K. Arrow indicates experimental oxygen pressure of 6.58x10^{-4} atm used in references 1 and 2.

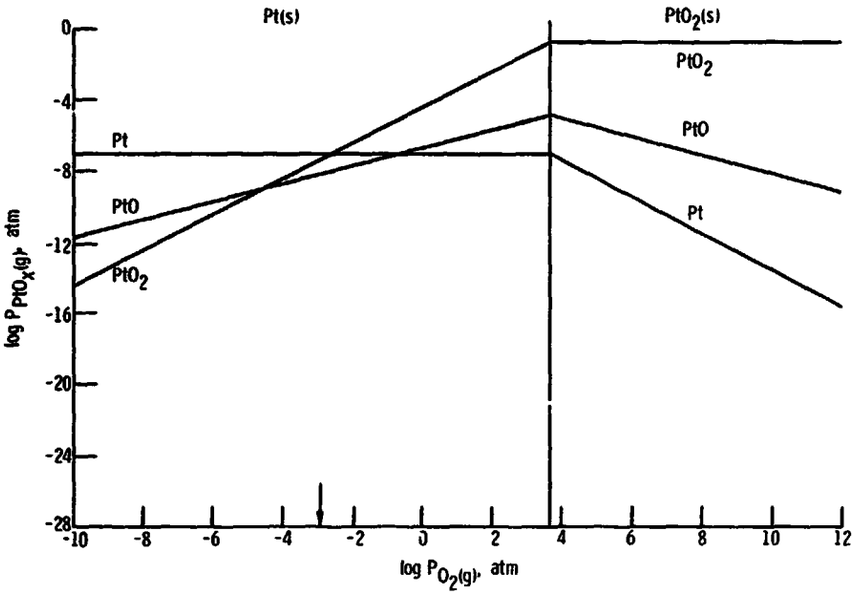

Figure 10. - Equilibrium thermochemical diagram for the platinum - oxygen system at 2000 K. Arrow indicates experimental oxygen pressure of 6.58×10^{-4} atm used in references 1 and 2.

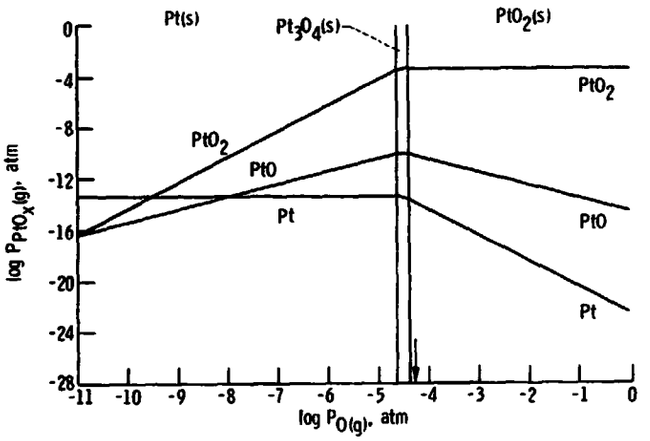

Figure 11. - Equilibrium thermochemical diagram for the platinum-atomic oxygen system at 1400 K. Arrow indicates experimental oxygen atom partial pressure of 4.61×10^{-5} atm used in reference 2.

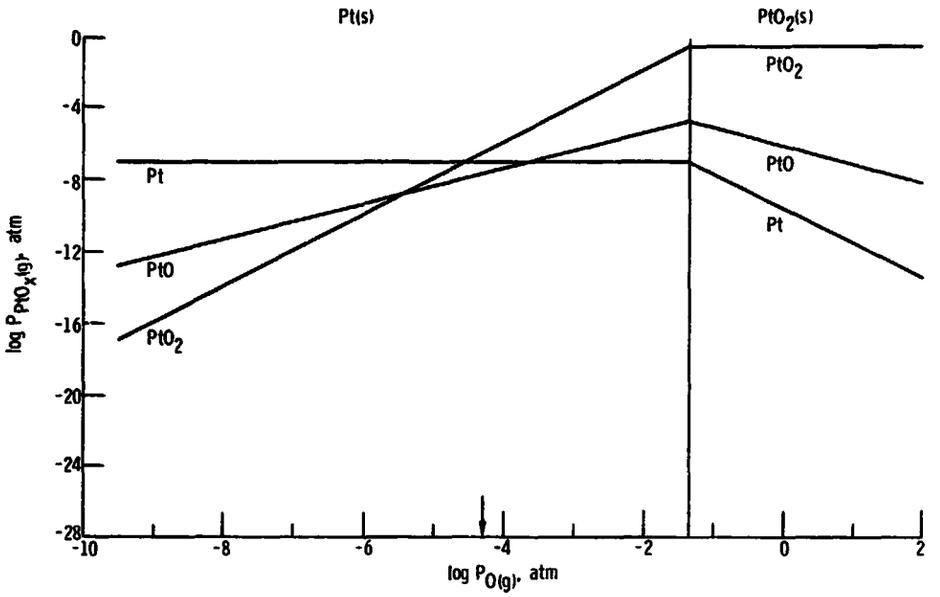

Figure 12. - Equilibrium thermochemical diagram for the platinum-atomic oxygen system at 2000 K. Arrow indicates experimental oxygen atom partial pressure of 4.61×10^{-5} atm used in reference 2.

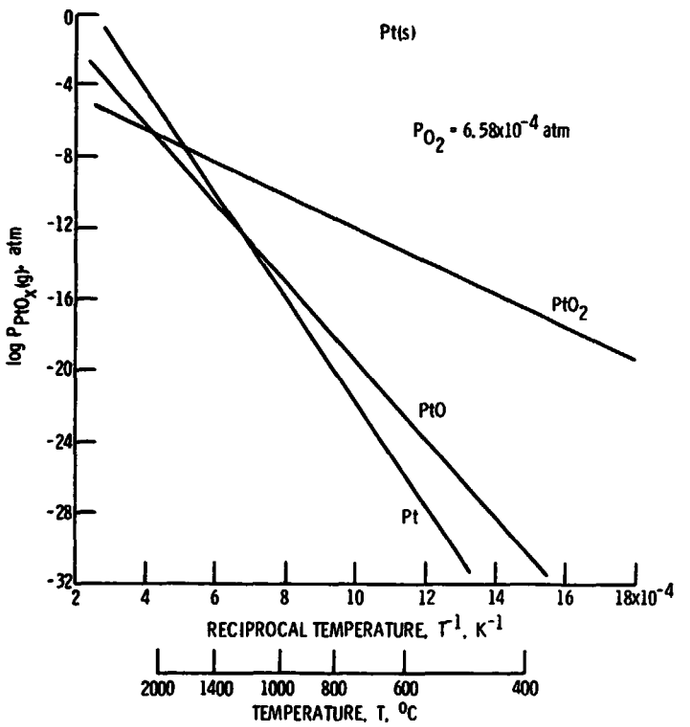

Figure 13. - Equilibrium vapor pressures of various molecules of the platinum-oxygen system over Pt(s) vs T^{-1} under an oxygen pressure of 6.58×10^{-4} atm.

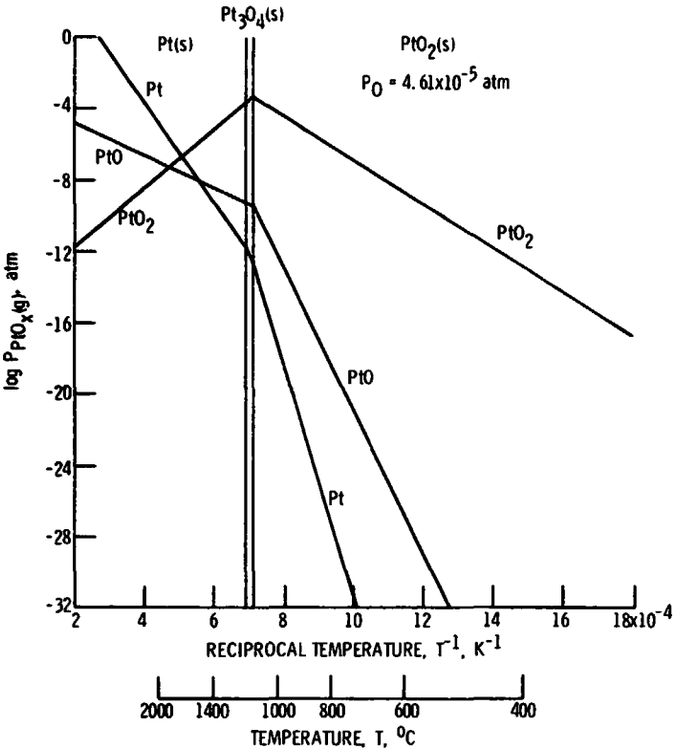

Figure 14. - Equilibrium vapor pressures of various oxide species of the platinum-atomic oxygen system vs T^{-1} under an oxygen atom partial pressure of $4.61x10^{-5}$ atm.

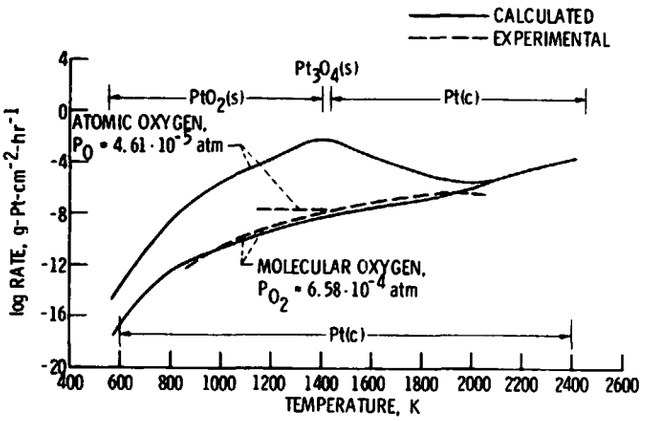

Figure 15. - Experimental and calculated rates of oxidative vaporization of platinum in partially atomic and molecular oxygen.

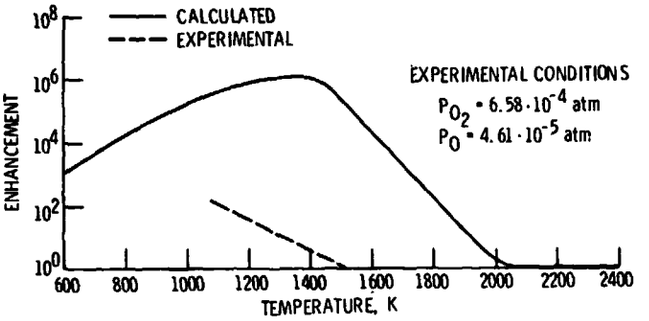

Figure 16. - Enhancement of oxidative vaporization of platinum in partially atomic oxygen.

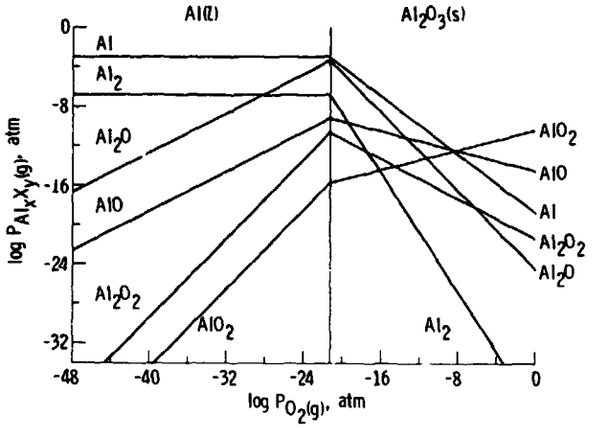

Figure 17. - Equilibrium thermochemical diagram for the aluminum-oxygen system at 1800 K.

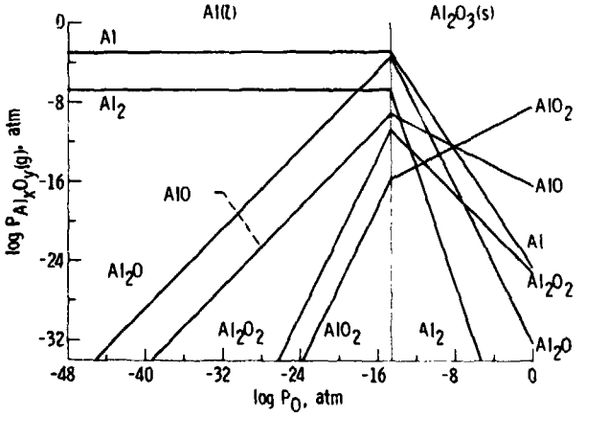

Figure 18. - Equilibrium thermochemical diagram for the aluminum - atomic oxygen system at 1800 K.

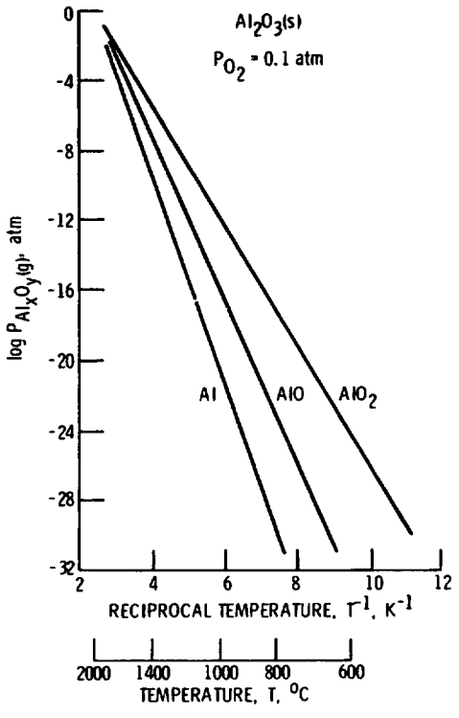

Figure 19. - Equilibrium vapor pressures of various oxide species of the aluminum-oxygen system over $Al_2O_3(s)$ vs T^{-1} under an oxygen pressure of 0.1 atm.

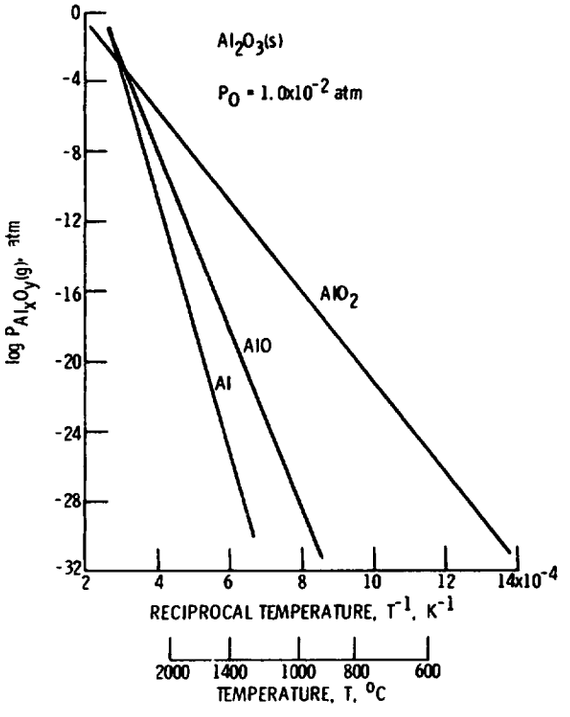

Figure 20. - Equilibrium vapor pressures of various molecules of the aluminum-atomic oxygen system vs T^{-1} under an oxygen atom partial pressure of 1.0×10^{-2} atm.

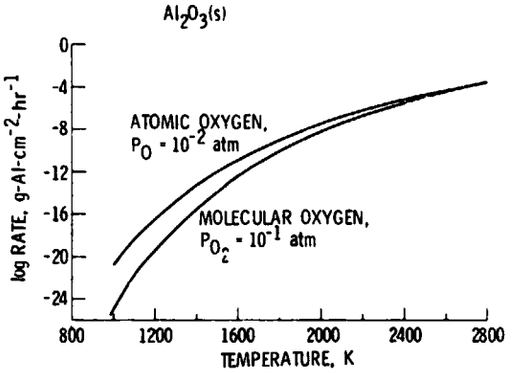

Figure 21. - Calculated rates of oxidative vaporization of Al_2O_3 in partially atomic and molecular oxygen.

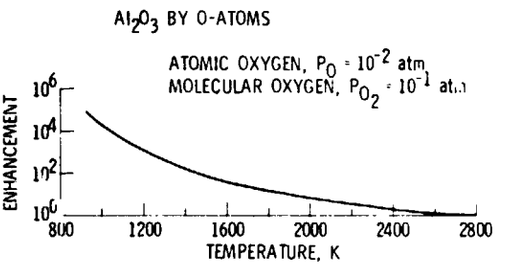

Figure 22. - Calculated enhancement of oxidative vaporization of Al_2O_3 in partially atomic oxygen.

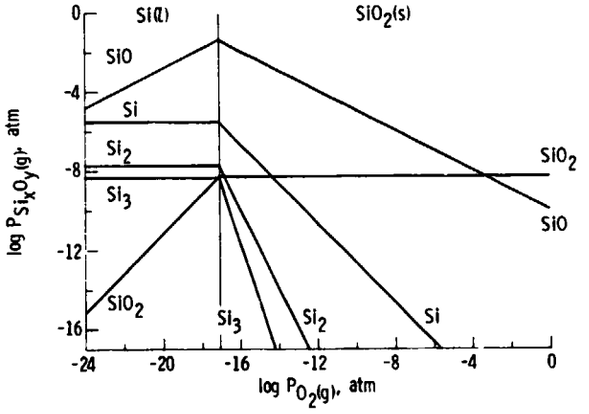

Figure 23. - Equilibrium thermochemical diagram for the silicon-oxygen system at 1800 K.

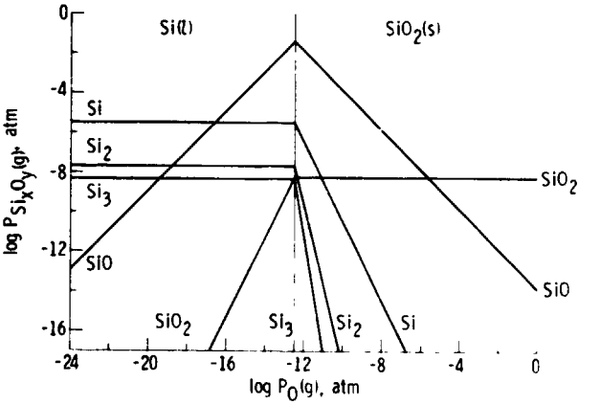

Figure 24. - Equilibrium thermochemical diagram for the silicon-atomic oxygen system at 1800 K.